remote sensing

MDPI

Article

Spatiotemporal Variations in Snow and Glacier Components and Associated Hazard Susceptibility Along the China–Kyrgyzstan Engineering Corridor in the Western Tianshan Mountains

Kun Zhang [1], Hongliang Li [2], Yanhu Mu [2], Yaozheng Luan [3], Fengchen Yu [2] and Puyu Wang [2,*]

[1] School of Civil Engineering, Northwest Minzu University, Lanzhou 730030, China; zhangkun@xbmu.edu.cn
[2] State Key Laboratory of Cryospheric Science and Frozen Soil Engineering, Northwest Institute of Eco-Environment and Resources, Chinese Academy of Sciences, Lanzhou 730000, China; lihongliang@nieer.ac.cn (H.L.); muyanhu@lzb.ac.cn (Y.M.); yufengchen@nieer.ac.cn (F.Y.)
[3] CCCC Highway Consultants Co., Ltd., Beijing 100088, China; luanyaozheng@ccccltd.cn
* Correspondence: wangpuyu@lzb.ac.cn

Highlights

What are the main findings?

- Multi-source remote sensing reveals reductions in glacier area and number and glacial-lake expansion along the China–Kyrgyzstan engineering corridor, while snow cover shows relatively stable interannual variability.
- Between 2002 and 2022, glacier number decreased by 66 and total glacier area decreased by 24.12 km^2 (18.28%), while between 1990 and 2018, both glacial-lake number and total area increased by more than 17%.

What are the implications of the main findings?

- Weighted overlay and fixed thresholds classified about 80% of the assessed corridor buffer as moderately or highly susceptible to snow- and glacier-related hazards.
- The sections located 35–64 km and 92–101 km from the highway starting point should be prioritized for targeted monitoring and field investigation.

Abstract

The China–Kyrgyzstan engineering corridor in the western Tianshan Mountains is an important route for transboundary transportation infrastructure. Climate-driven changes in snow cover, glaciers, and glacial lakes may affect highway construction and long-term operational safety. This study integrates a 500 m MOD09GA-derived snow-cover product, a passive microwave snow-depth product with a grid spacing of 25 km and glacier and glacial-lake inventories to examine changes in snow cover (2001–2020), snow depth (2000–2018), glaciers (2002–2022), and glacial lakes (1990–2018) within a 10 km buffer on each side of the highway. A weighted linear overlay method combined the snow, glacier, and glacial-lake layers to assess integrated hazard susceptibility, while historical hazard records provided regional context for interpreting potential hazard processes. The results show that: (1) The snow-covered area ratio remained relatively stable during 2001–2020, averaging 10.33%, whereas annual maximum snow depth and annual mean snow depth both declined significantly during 2000–2018, ranging from 6.6 to 22 cm and from 1.66 to 3.36 cm, respectively. Seasonal snow conditions suggest greater potential for avalanches in winter and snowmelt floods in spring and summer. (2) In 2002, 337 glaciers were identified within the 10 km corridor buffer; glaciers with areas smaller than 0.5 km^2 accounted for 75% of the glacier number. Between 2002 and 2022, the glacier number decreased by 66, while total glacier area decreased by 24.12 km^2 (18.28%), equivalent to an average annual loss of 0.914% of the 2002 area. (3) In 2018, 77 glacial lakes were identified within the 10 km corridor

Check for updates

Academic Editors: Ulrich Kamp, Richard Gloaguen and Pengfeng Xiao

Received: 15 September 2026
Revised: 8 November 2026
Accepted: 27 November 2026
Published: 28 November 2026

Copyright: © 2026 by the authors. Licensee MDPI, Basel, Switzerland. This article is an open access article distributed under the terms and conditions of the Creative Commons Attribution (CC BY) license.

buffer; glacial lakes with areas smaller than 0.5 km^2 accounted for approximately 91% of the glacial-lake number. Between 1990 and 2018, both lake number and total area increased by more than 17%. Ten regional glacial lake outburst flood (GLOF) events were documented during 1974–2019, providing context for potential hazard processes rather than evidence of direct impacts on the highway. (4) Moderate susceptibility predominates, covering approximately 78% of the study area, whereas high-susceptibility zones cover approximately 2%. High-susceptibility zones are concentrated mainly along highway sections approximately 35–64 km and 92–101 km from the starting point, which warrant priority field investigation and monitoring to identify relevant hazard sources and propagation pathways. These findings provide screening-level guidance for corridor-scale hazard assessment and monitoring prioritization, while highway engineering safety requires further evaluation through field investigations, geotechnical engineering assessments, and verification through monitoring.

Keywords: China–Kyrgyzstan engineering corridor; snow-cover change; glacier change; glacial-lake expansion; hazard susceptibility assessment

1. Introduction

Rapid warming in the Central Asian Tianshan Mountains has been accompanied by changes in snow-cover patterns, widespread reductions in glacier area and number, and glacial-lake expansion, with implications for snow- and glacier-related hazards [1]. The Tianshan Mountains are highly sensitive to climate change and have experienced a warming and wetting trend since the early 21st century, although temperature and precipitation exhibit substantial variability [2,3]. More frequent and intense climatic extremes may further alter the conditions that trigger avalanches, snowmelt floods, and glacial lake outburst floods (GLOFs), potentially threatening transportation infrastructure and ecosystems in high-mountain regions [4].

Transportation infrastructure, particularly transboundary highways, supports regional economic connectivity and international exchange. Its safe construction and reliable long-term operation are therefore essential to regional development and cross-border trade. Previous studies have shown that changes in snow and ice conditions can affect the stability and operation of transportation infrastructure in high-mountain regions. Changes in snow accumulation and melt can contribute to snow blockage and flooding, while glacier changes may alter meltwater supply and slope stability. Freeze–thaw processes can additionally cause frost heave and thaw settlement of roadbeds [5,6]. At high-elevation passes and in deeply incised valleys, complex terrain may channel rapidly developing snow- and glacier-related hazards toward roads and other infrastructure [7,8]. Studies of the Qinghai–Tibet Railway and Highway have highlighted the challenges that changing snow cover, glacier, and frozen-ground conditions pose to infrastructure construction and operation in cold regions [9]. Compared with the Tibetan Plateau, the Tianshan Mountains have received less systematic attention regarding changes in snow cover, glaciers, and glacial lakes and their implications for transportation infrastructure. Integrated hazard investigations and susceptibility assessments remain particularly limited along transboundary transportation corridors.

The Baryskoon–Bedel Border Port Highway in Kyrgyzstan (hereafter, the China–Kyrgyzstan Highway) traverses the high-mountain terrain of the western Tianshan Mountains and forms part of a transboundary transportation corridor linking Issyk-Kul Region in Kyrgyzstan with Kizilsu Kyrgyz Autonomous Prefecture in Xinjiang, China. The approximately 150 km highway is a key infrastructure project supporting China–Kyrgyzstan connectivity under the Belt and Road Initiative. From north to south, it crosses the Baryskoon,

Suuk, and Ashuu-Suu mountain passes and the Karasay Valley, reaches the Bedel Border Port checkpoint, and links to the road network serving Akqi County in Xinjiang. The highway is expected to shorten the transportation distance between China and Kyrgyzstan by approximately 500 km and reduce freight travel time by more than 12 h, supporting bilateral trade, regional economic cooperation, and transboundary tourism.

The highway traverses rugged mountain terrain with high-elevation passes, deeply incised valleys, and substantial elevation differences. Snow cover, glaciers, and glacial lakes occur along the route, making the corridor potentially susceptible to multiple snow- and glacier-related hazards. Changes in these components and the hazards associated with them may affect both construction safety and long-term highway operation. Assessing changes in snow cover, glaciers, and glacial lakes, together with historical hazard records and spatial susceptibility, can help identify highway sections requiring further investigation. Such assessments can guide monitoring priorities and inform subsequent site-specific engineering design and hazard mitigation.

Recent studies have documented rapid glacial-lake expansion and substantial downstream exposure to potential GLOFs, highlighting the need to consider both evolving hazard sources and exposed populations and infrastructure [10,11]. Investigations in the northern Tian Shan have further shown that small, short-lived lakes can generate damaging floods through changes in meltwater supply, buried-ice degradation, and drainage conditions [12,13]. A reconstruction of the 2023 Sikkim disaster demonstrates how slope failure, lake impact waves, dam breaching, and sediment entrainment can form a cascade with severe downstream infrastructure impacts [14]. Regional assessments have also examined glacial-lake changes and GLOF risk across the Tianshan Mountains [15]. Together, these studies provide a foundation for understanding hazard mechanisms and regional exposure.

Despite growing attention to changes in snow cover, glaciers, and glacial lakes and their associated hazards in high-mountain regions, integrated assessments linking these changes to hazard susceptibility along the China–Kyrgyzstan engineering corridor remain limited. Analyses of individual components alone provide an incomplete basis for screening a corridor potentially affected by multiple snow- and glacier-related hazards. This study therefore aims to (1) characterize changes in snow-covered area ratio, snow depth, glaciers, and glacial lakes along the corridor over their respective analysis periods; (2) identify potentially susceptible areas by jointly considering the spatial distributions of these components, terrain conditions, and proximity to the highway; and (3) identify highway sections requiring priority attention for hazard monitoring and further site-specific investigation. To achieve these objectives, we establish a 10 km buffer on each side of the highway centerline and integrate a 500 m MOD09GA-derived snow-cover product, a passive microwave snow-depth product with a grid spacing of 25 km, glacier and glacial-lake inventories, and historical hazard records to characterize changes in these components and assess integrated hazard susceptibility. The contribution of this study lies in bringing these multiple sources of information into a common corridor-scale assessment, thereby connecting the analysis of snow cover, glacier, and glacial-lake changes with the spatial prioritization of hazard screening. The results provide a basis for identifying priority highway sections and guiding subsequent field surveys, monitoring, and engineering assessments.

2. Study Area

The China–Kyrgyzstan engineering corridor is located in the southeastern part of Issyk-Kul Region, Kyrgyzstan, in the western Tianshan Mountains, and forms an important transboundary transportation link between Kyrgyzstan and Xinjiang, China (Figure 1a). Elevations generally increase from northwest to southeast, ranging from approximately

2500 to 4200 m a.s.l., with local peaks exceeding 4500 m a.s.l. The landscape is characterized by rugged alpine terrain and deeply incised valleys.

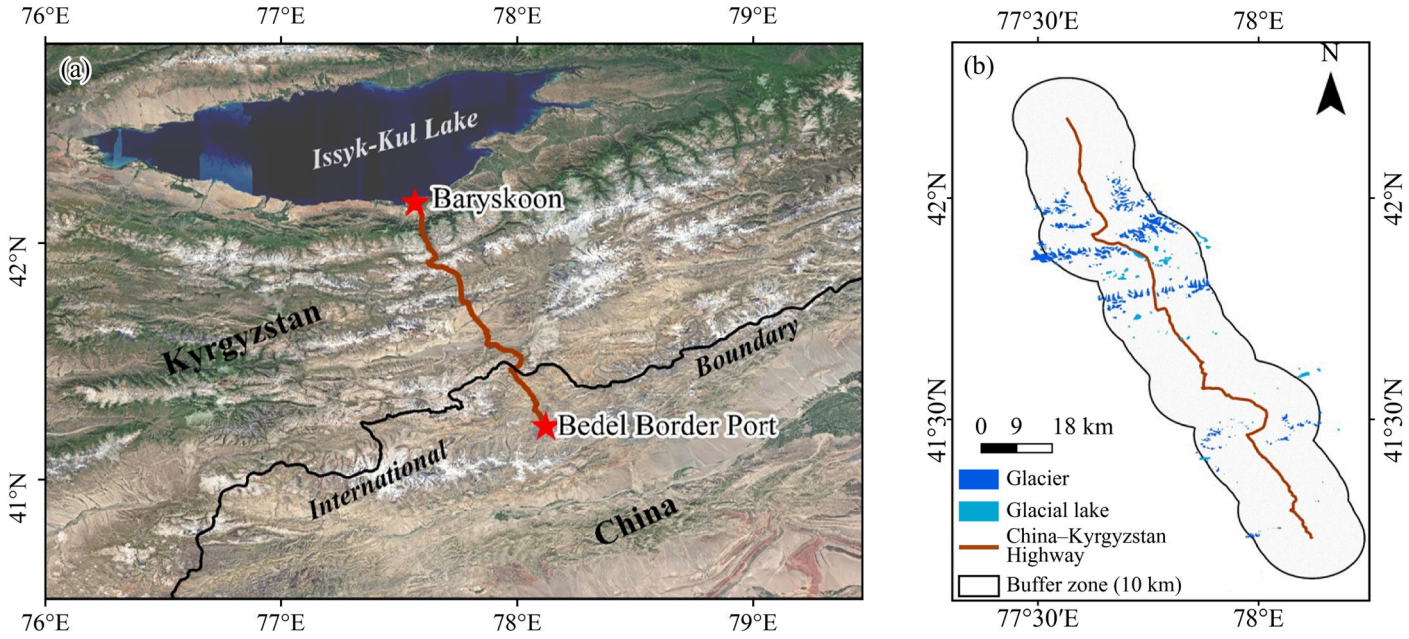

Figure 1. Study area: (**a**) geographic location of the Baryskoon–Bedel Border Port Highway; (**b**) highway route, 10 km buffer zone, and distribution of glacier and snow resources.

The study area was delineated as a 10 km buffer on each side of the highway centerline (Figure 1b). This buffer provides a consistent spatial framework for compiling snow cover, glacier, and glacial-lake information and conducting corridor-scale hazard susceptibility screening. It defines the scope of the present assessment rather than a physically determined limit of hazard propagation. Sources outside the buffer may still affect the highway through connected upstream catchments and river channels.

The region has a continental alpine climate, with relatively abundant precipitation, low temperatures, and low evaporation. Snowfall occurs over a period of approximately 5–7 months each year, and snow depth generally increases with elevation [16]. Orographic uplift contributes to spatial variability in snowfall, while wind redistribution can promote localized snow accumulation at mountain passes and on windward slopes. Streamflow is sustained primarily by glacier ablation and seasonal snowmelt, with rapid increases in snowmelt runoff during spring warming. The area has complex lithology, with locally weathered rock masses and unconsolidated deposits. Snow accumulation and freeze–thaw processes may contribute to avalanche formation and slope instability, depending on local snowpack, terrain, and ground conditions.

3. Data and Methods

3.1. Analysis of Snow and Glacier Components

Snow cover information was obtained from the Belt and Road Snow Area Proportion Daily Data Product Dataset, distributed by the National Cryosphere Desert Data Center (Table 1). This product is derived from MOD09GA surface reflectance and provides daily data at a spatial resolution of 500 m. The data producers retrieved fractional snow cover using a multivariate adaptive regression splines (MARS) model incorporating CGLS-LC100 land-cover information, with Landsat-8-derived fractional snow cover used as reference data. We used the product for 2001–2020 and extracted corridor data within a 10 km buffer on each side of the highway. The regional snow-covered area ratio (*SCAR*) was calculated

as the number of snow-covered pixels in each image divided by the total number of pixels within the study area:

$$SCAR = \left(\frac{N_{snow}}{N_{total}} \right) \times 100\% \quad (1)$$

where N_{snow} is the number of pixels classified as snow-covered within the study area, and N_{total} is the total number of pixels within the study area.

Table 1. Main datasets used to characterize snow, glacier, and glacial-lake changes along the China–Kyrgyzstan engineering corridor.

Dataset Type	Analysis Period	Source
Snow depth	2000–2018	Global long-term daily snow-depth dataset (DOI: 10.11888/Snow.tpdc.270925)
Snow cover	2001–2020	Daily fractional snow-cover dataset for the Belt and Road region (DOI:10.12072/ncdc.nieer.db6622.2024, 2 November 2026)
Glacier outlines	2002	Randolph Glacier Inventory (RGI v7.0)
Glacier outlines	2022	Glacier inventory of four Central Asian countries ([17])
Glacial-lake outlines	1990 and 2018	Glacial lake inventory of High Mountain Asia (DOI: 10.12072/casnw.064.2019.db, 2 November 2026)

Snow depth was obtained from the Long-term Series of Daily Global Snow Depth Dataset (1980–2018), distributed by the National Tibetan Plateau Data Center (DOI: 10.11888/Snow.tpdc.270925). The dataset provides daily snow depth estimates retrieved from SMMR, SSM/I, and SSMIS passive microwave observations using a dynamic brightness-temperature-gradient algorithm, with an original grid spacing of approximately 25 km (Table 1). We resampled the data to a 0.25° × 0.25° geographic grid using nearest-neighbor resampling and extracted the 2000–2018 records within the 10 km buffer on each side of the highway. Temporal trends in the annual snow-covered area ratio, annual maximum snow depth, and annual mean snow depth were estimated using linear regression against calendar year. Statistical significance was assessed using a two-sided test of whether the regression slope differed from zero. Trends were considered statistically significant at $p < 0.05$. The snow-cover and snow-depth trends were evaluated over their respective observation periods of 2001–2020 and 2000–2018.

Glacier changes were assessed using glacier outlines from the Randolph Glacier Inventory (RGI v7.0) for the baseline epoch of 2002 and the inventory published by [17] for the recent epoch (Table 1). Although the latter dataset covers four Central Asian countries during 2022–2023, the glacier outlines along the China–Kyrgyzstan Highway used in this study correspond to 2022. This inventory was produced using a convolutional neural network–Transformer framework followed by manual inspection and correction. The two inventories were used to quantify changes in glacier number, area, and size distribution along the corridor during 2002–2022.

Glacial-lake data were obtained from the Glacial Lake Inventory of High-Mountain Asia, distributed by the National Cryosphere Desert Data Center (DOI: 10.12072/casnw.064.2019.db). The inventory provides lake outlines for the nominal epochs of 1990 and 2018, derived from Landsat imagery using NDWI-assisted delineation and manual visual interpretation (Table 1). We used two existing outlines to assess changes in glacial-lake number, area, and size distribution within the highway buffer during 1990–2018.

The analysis periods reflect the coverage of the data used in this study and the observation epochs of the selected inventories: 2000–2018 for snow depth, 2001–2020 for snow-covered area ratio, 2002–2022 for glacier changes, and 1990–2018 for glacial lake

changes. In particular, the different periods used for glacier and glacial-lake change assessments arise from differences in the observation epochs of the public inventories. Each component was therefore analyzed over its respective analysis periods.

3.2. Compilation of Snow and Glacier Hazard Database

Historical hazard records were compiled to characterize snow- and glacier-related hazards that may affect the China–Kyrgyzstan engineering corridor. Snowmelt-flood and GLOF records were obtained from the historical flood-disaster dataset for the Tibetan Plateau and surrounding mountain regions (1950–2023), whereas information on surge-type glaciers was obtained from the inventory of surge-type glaciers in High Mountain Asia. Regional avalanche cases and glacial-lake investigations provided supplementary information for analyzing potential hazard processes.

The compiled records include five snowmelt-flood events in Akqi County during 1983–2011 and ten GLOF events involving seven lakes during 1974–2019. All ten GLOF events occurred outside the highway's 10 km buffer, approximately 19–56 km from its boundary. These events provide regional context for interpreting potential hazard processes. The surge-glacier inventory identifies four surge-type glaciers in the Kungey Mountains outside the highway's 10 km buffer, whereas none were identified within the buffer. These glaciers are counted as potential hazard sources rather than independent disaster events. The available avalanche information primarily describes regional cases and potentially susceptible locations.

The representation of hazard types is uneven because the available information differs in spatial coverage, observation period, and reporting completeness. Therefore, historical events, surge-type glaciers, and potentially susceptible locations are distinguished rather than combined into a single event count. Thus, historical records were not directly included in the susceptibility index.

3.3. Snow and Glacier Hazard Susceptibility Assessment

The susceptibility assessment was conducted in two stages within a 10 km buffer along the highway. First, separate susceptibility maps were prepared for hazards associated with glacial lakes, glaciers, and snow. Second, the susceptibility classes in each component map were converted to numerical scores, and the three maps were combined by weighted linear overlay to calculate an integrated susceptibility index. The indicators considered for each component are summarized in Table 2. The assessment used glacier outlines from 2022, glacial lake outlines from 2018, and snow cover and snow depth data for the respective periods specified in Section 3.1. Because the input datasets represent different years and observation periods, the resulting maps provide a relative susceptibility assessment for screening along the China–Kyrgyzstan Highway and do not represent conditions at a single point in time.

Each component was classified separately into low, moderate, and high susceptibility according to its own indicator criteria. These classes were then assigned scores of 1, 2, and 3, respectively, for the integrated assessment. The three component maps were combined by weighted overlay in ArcMAP 10.3. Based on expert consultation [18–20], weights of 0.40, 0.30, and 0.30 were assigned to the glacial lake, glacier, and snow components, respectively. The glacial lake component received a slightly higher weight because glacial lakes can store water and release it suddenly during an outburst, potentially affecting downstream infrastructure. The integrated susceptibility index was calculated as follows:

$$H = 0.4L + 0.3G + 0.3S \quad (2)$$

where L, G, and S are the susceptibility scores for the glacial lake, glacier, and snow components, respectively, expressed on a common scale. Higher H values indicate greater relative integrated susceptibility under the adopted weighting scheme.

Table 2. Indicators considered in the susceptibility assessment for each hazard component.

Component	Indicators Considered	Role in the Assessment
Glacial lake hazards (L)	Lake area, distance to the highway, and lake type	Lake area characterizes the size of the potential hazard source, and distance indicates its proximity to the highway. All lakes included in the assessment were moraine-dammed; lake type was therefore recorded as a descriptive attribute and was not assigned a separate score.
Glacier hazards (G)	Glacier area, distance to the highway, slope, and aspect	Glacier area characterizes the size of the potential hazard source, distance indicates its proximity to the highway, and slope and aspect describe the terrain conditions.
Snow-related hazards (S)	Snow-covered area ratio, snow depth, slope, and aspect	The snow-covered area ratio and snow depth characterize snow conditions, while slope and aspect describe the terrain where snow accumulates and snow-related hazards may develop.

The integrated index was classified into low, moderate, and high susceptibility using fixed thresholds. The area of each class was expressed as a proportion of the total area within the highway buffer for which the index was calculated. Historical hazard records were used to interpret regional hazard processes and were neither included directly in the index calculation nor used for independent quantitative validation. In addition, "hazard" refers to potentially damaging processes or events in this study, whereas "susceptibility" describes the relative spatial propensity indicated by the component-based assessment. Because infrastructure exposure and vulnerability were not systematically quantified, the integrated index and its classes represent relative susceptibility rather than risk estimates or probabilities of hazard occurrence.

3.4. Uncertainty Analysis

All snow cover, glacier, and glacial-lake inputs were obtained from publicly available datasets. We used the published snow products and inventory outlines without independently retrieving snow parameters or delineating glacier and glacial-lake boundaries. Where available, we used the validation results and mapping errors reported by the data producers to characterize input-data uncertainty. The snow-depth dataset has an original spatial resolution of approximately 25 km. Resampling to a 0.25° × 0.25° grid does not improve its effective spatial resolution; therefore, it primarily represents regional snow conditions and has limited capacity to characterize local snow depth. Although the 500 m snow-cover product provides finer spatial information, it may still be affected by mixed pixels, terrain shadow, and limitations in the applicability of the MARS model.

The accuracy of mapped glacier outlines and estimates of glacier change is affected by boundary delineation errors and differences in glacier identification and subdivision criteria among inventories. Ref. [17] reported an overall area uncertainty of 4.76% for the glacier inventory of four Central Asian countries. The glacial-lake inventory reports a boundary-position uncertainty of approximately ±15 m and mean relative area errors of 13.5% and 13.2% for 1990 and 2018, respectively.

Temporal inconsistency among the input datasets introduces additional uncertainty into the integrated susceptibility assessment. The assessment combines the mean snow-covered area ratio over the observation period specified in Section 3.1 with glacier outlines from 2022 and glacial-lake outlines from 2018. The inputs retain their original temporal references. Historical hazard records were used only for regional process interpretation and were not directly included in the index. These temporal differences may affect the mapped distribution and overlap of potential hazard sources. Changes in glacier and lake boundaries after their inventory dates may alter component contributions, while the multi-year snow-cover mean smooths interannual variability and may not represent conditions in a particular year. Consequently, areas where sources have emerged, disappeared, or changed substantially may be assigned different susceptibility classes if temporally aligned data are used. The identified high-susceptibility zones therefore represent screening priorities based on the available datasets, rather than conditions at a single common date. Their sensitivity to temporal alignment has not been quantified and requires reassessment using updated, temporally consistent inputs. Under the fixed weights in Equation (2), changes in the component scores affect the integrated susceptibility index (ΔH) according to:

$$\Delta H = 0.4\Delta L + 0.3\Delta G + 0.3\Delta S \quad (3)$$

where ΔL, ΔG, and ΔS are changes in the glacial-lake, glacier, and snow scores, respectively. With the other scores held constant, a one-unit change in the glacial-lake score changes H by 0.4, compared with 0.3 for the same change in the glacier or snow score.

4. Results and Discussion

4.1. Changes in Snow and Glacier Components Along the Highway

From 2001 to 2020, the snow-covered area ratio within the 10 km buffer increased slightly, at a statistically insignificant rate of 0.01% a^{-1}. Annual values ranged from 8.91% to 11.99%, with a period mean of 10.33% (Figure 2). During 2000–2018, annual maximum snow depth ranged from 6.6 to 22 cm, with a mean of 12.54 cm, whereas annual mean snow depth ranged from 1.66 to 3.36 cm, with a period mean of 2.16 cm (Figure 3a). Both measures declined significantly over this period. Annual maximum snow depth decreased at 0.52 cm a^{-1} ($p < 0.01$), approximately ten times the rate of decline in annual mean snow depth (0.05 cm a^{-1}, $p < 0.05$). Snow depth was generally high during 2000–2004, with annual maxima exceeding 20 cm in some years, followed by an overall decline with interannual fluctuations during 2005–2013. Although snow depth partially recovered during 2014–2018, it remained approximately half its value in 2000. The seasonal snow-depth cycle was distinctly unimodal: snow accumulation began in September–October, snow depth peaked in February, declined markedly from March to May, and reached its minimum in August (Figure 3b).

According to RGI v7.0, 337 glaciers with a total area of 131.95 km^2 were present within the 10 km buffer along the China–Kyrgyzstan Highway in 2002 (Figure 4a). Glaciers smaller than 0.5 km^2 accounted for 75% of the total number (252 glaciers), including 129 glaciers smaller than 0.1 km^2. 28 glaciers were larger than 1 km^2 and 6 glaciers were larger than 2 km^2. Within the 2 km buffer zone, 71 glaciers were identified, with a mean glacier area of 0.39 km^2. Between 2002 and 2022, the number of glaciers within the 10 km buffer decreased from 337 to 271. Total glacier area decreased from 131.95 km^2 to 107.83 km^2, a reduction of 24.12 km^2 (18.28%). This corresponds to an average area loss of 1.206 km^2 a^{-1}, or 0.914% of the 2002 area per year (Figure 4a).

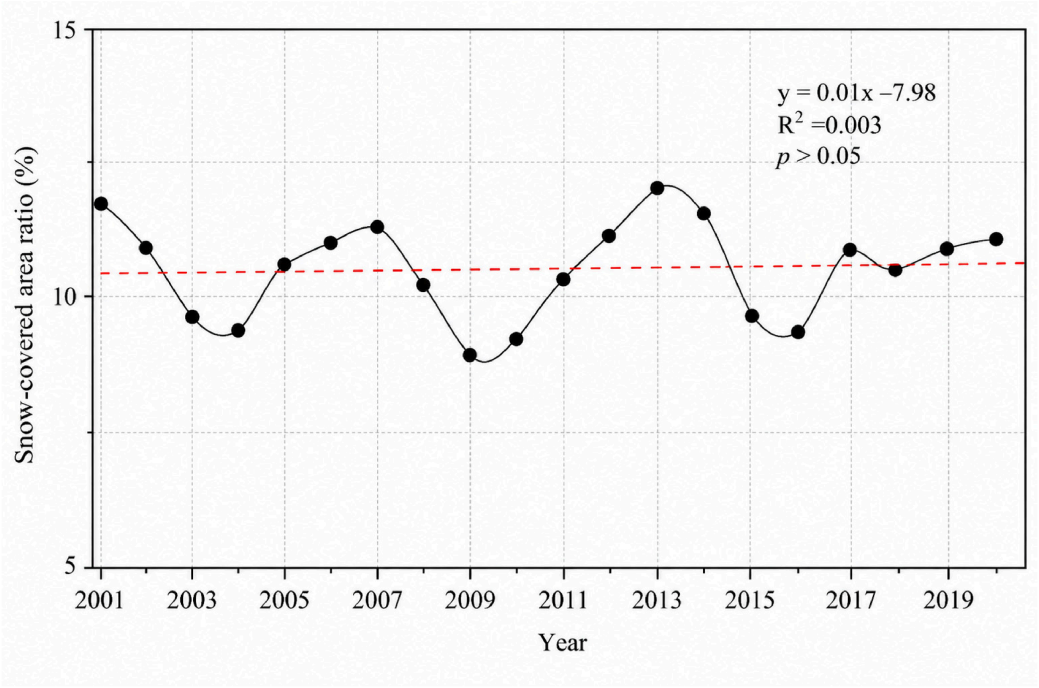

Figure 2. Variation in the snow-covered area ratio within the 10 km buffer zone along the China–Kyrgyzstan Highway from 2001 to 2020.

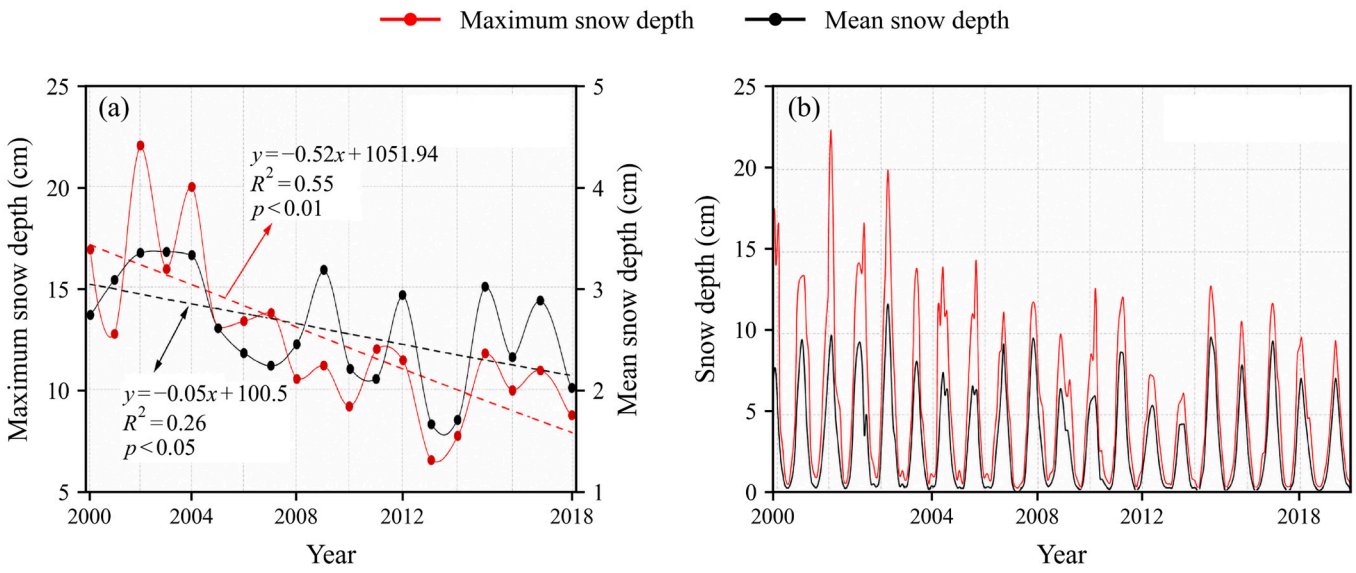

Figure 3. Variation in snow depth within the 10 km buffer zone along the China–Kyrgyzstan Highway from 2000 to 2018: (**a**) annual scale; (**b**) monthly scale.

In 2018, 77 glacial lakes covering a total area of 10.46 km^2 were identified within the 10 km buffer (Figure 4b). Of these, 70 (approximately 91%) were smaller than 0.5 km^2, including 58 (approximately 75%) smaller than 0.1 km^2; the remaining 7 glacial lakes exceeded 0.5 km^2. Within the 2 km buffer, 31 glacial lakes were identified, with a mean area of 0.11 km^2. 2 lakes adjacent to the highway, GL077727E41869N and GL077715E41879N, had areas of 0.921 and 0.166 km^2, respectively. Between 1990 and 2018, the number increased by 13 (approximately 20%), and total lake area increased by 17%. Within the 2 km buffer, total glacial-lake area increased by 0.419 km^2. Over the same period, the areas of GL077727E41869N and GL077715E41879N increased by 0.069 and 0.023 km^2, respectively.

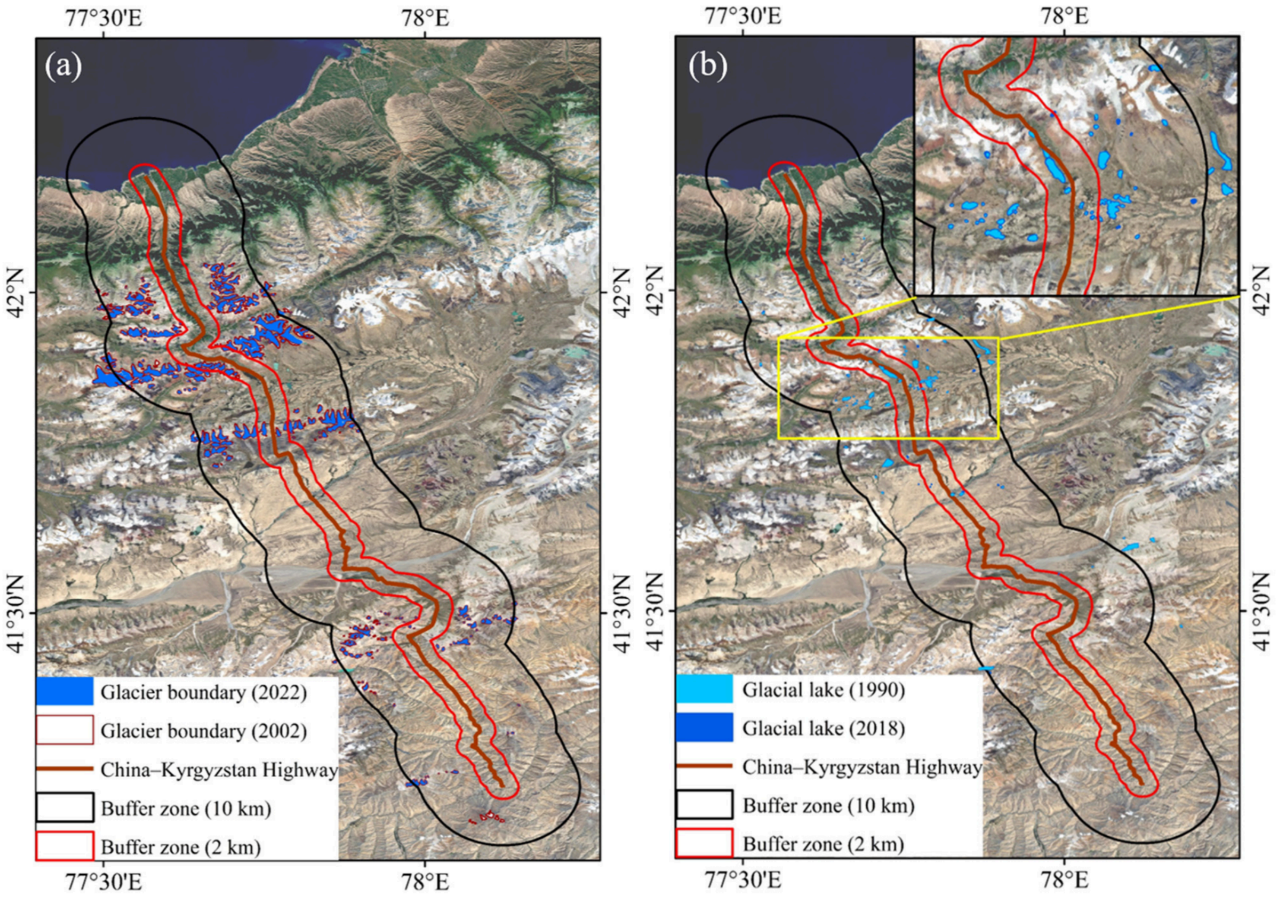

Figure 4. Changes in glaciers and glacial lakes within the 10 km buffer zone along the China–Kyrgyzstan Highway: (**a**) glacier changes from 2002 to 2022; (**b**) glacial-lake changes from 1990 to 2018.

4.2. Historical Snow- and Glacier-Related Hazards in the Corridor and Surrounding Regions

Five snowmelt-flood events were recorded in Akqi County during 1983–2011, occurring in August 1983, on 30 and 31 July 1990, on 13 July 2006, and during 24–26 April 2011. These events damaged houses, farmland, crops, and embankments. The 2011 event caused direct economic losses of RMB 93.0274 million, including RMB 76.937 million from flood damage to three sections of Provincial Highway S306. These county-level records demonstrate that snowmelt floods can severely affect transportation infrastructure. However, the event locations relative to the study highway and their hydrological connectivity to it have not been verified. These records therefore provide regional context rather than direct evidence of flood impacts on the China–Kyrgyzstan engineering corridor. Regional avalanche information also identifies four potentially avalanche-prone locations along the North–South Alternative Road in the Fergana Mountains. These locations provide regional context and do not represent four avalanche events along the China–Kyrgyzstan Highway.

According to the inventory of surge-type glaciers in High Mountain Asia, no surge-type glaciers occur within the 10 km buffer zone along the China–Kyrgyzstan Highway. However, four surge-type glaciers are distributed in the Kungey Mountains on the northern shore of Issyk-Kul Lake in northeastern Kyrgyzstan (Table 3). These glaciers underwent surges during 1990–2016, with individual surge durations of approximately 3–9 years. G077183E42955N surged from 2007 to 2016, lasting approximately 9 years. These observations document regional glacier surging, but do not establish hazard propagation pathways or direct impacts on the study highway.

Table 3. Basic information on surge-type glaciers in the Kungey Mountains on the northern shore of Issyk-Kul Lake, northeastern Kyrgyzstan.

GLIMS ID	Longitude (°E)	Latitude (°N)	Area (km^2)	Surge Period			Evidence from Satellite Imagery and DEM Differencing
				Start	End	Duration (yr)	
G077249E43084N	77.25	43.085	5.4985	1999	2002	3	DEM differencing for 2000–2009 indicates surface uplift near the glacier terminus. Remote-sensing images from 9 September 1999 to 3 October 2002 show marked surface advance, development of teardrop-shaped moraines, and moraine displacement.
G077248E43020N	77.26	43.041	46.34	1990–1993	1996	3–6	Remote-sensing images from 1990 to 1996 show a 252 m terminus advance. DEM differencing for 2000–2016 indicates uplift in the receiving zone and marked lowering in the reservoir zone. The northern branch displaced the southern branch by 419 m; teardrop-shaped moraines developed.
G077183E42955N	77.18	42.955	23.345	2007	2016	9	DEM differencing for 2000–2016 indicates substantial glacier transfer by the southern branch from the reservoir zone toward the receiving zone. The southern branch displaced the northern branch by 218 m; teardrop-shaped moraines and extensive crevassing developed on all branches.
G077241E42927N	77.24	42.928	20.774	1996	2001	5	Remote-sensing images from 1996 to 2001 show a 782 m terminus advance. DEM differencing for 2000–2016 indicates uplift in the receiving zone and marked lowering in the reservoir zone. New crevasses developed across the glacier tongue, together with teardrop-shaped moraines.

The compiled GLOF records comprise ten events involving seven lakes during 1974–2019 (Table 4), including repeated outbursts from Angy Say. All ten events occurred outside the highway's 10 km buffer, at locations approximately 19–56 km from the buffer boundary. Most glacial lakes are classified as moraine-dammed, whereas the type of Suuk Tor remains unknown. These records illustrate regional GLOF processes; their inclusion does not establish hydrological connectivity to the study highway. The Toguz-Bulak outburst on 8 August 2019 provides a documented regional example of a glacier–lake–downstream flood cascade. Remote-sensing observations and field investigations linked lake expansion to increased summer glacier meltwater supply and identified buried-ice melt and surface subsidence within the moraine complex as contributing factors to dam destabilization. Following the breach, glacial lake area decreased from 0.021 to 0.002 km^2, with most of the stored water discharged within four hours (Figure 5). Floodwater entrained sediment and propagated downstream through the Tosor river system, damaging bridges and roads [12]. This case illustrates the connections among glacier meltwater supply, moraine degradation, lake drainage, and downstream infrastructure impacts. The documented damage concerns infrastructure within the affected river system and should not be interpreted as demonstrated damage to the study highway.

Table 4. Information on GLOF events.

Glacial Lake Name	Lake Type	Main Cause	Outburst Date
Angy Say	Moraine-dammed lake	-	14 June 1974
Angy Say	Moraine-dammed lake	-	17 June 1975
Angy Say	Moraine-dammed lake	-	25 June 1980
Angy Say	Moraine-dammed lake	-	14 July 1980
Suuk Tor	Unknown	-	24 June 1988
Kashka-Suu	Moraine-dammed lake	Subglacial drainage pathway	-
Western Zyndan	Moraine-dammed lake	Buried-glacier melt	24 July 2008
Jeruy	Moraine-dammed lake	Subglacial drainage pathway	15 August 2013
Karateke	Moraine-dammed lake	-	17 July 2014
Toguz-Bulak	Moraine-dammed lake	Subglacial drainage pathway	8 August 2019

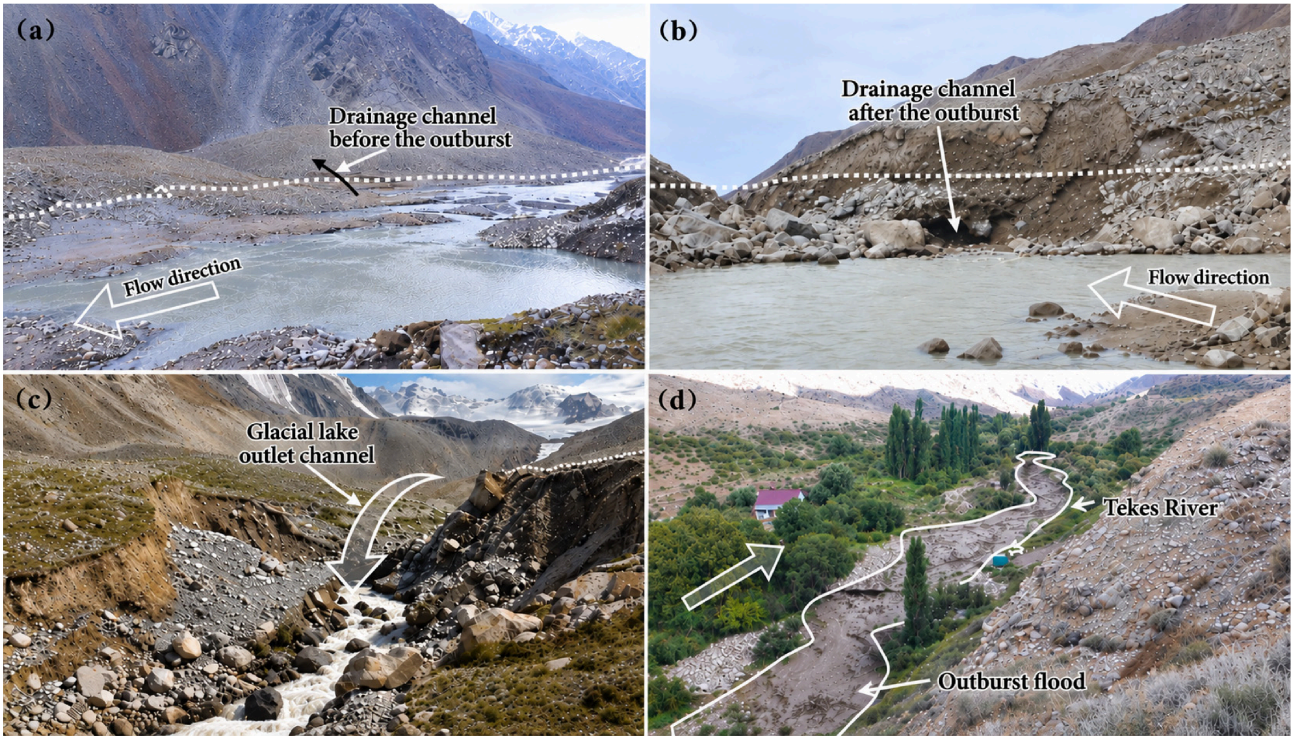

Figure 5. Conditions before and after the GLOF at Toguz-Bulak glacial lake; modified from [21]. (**a**) Drainage channel before the outburst; (**b**) drainage channel after the outburst; (**c**) glacial lake outlet channel; (**d**) outburst flood routing toward the Tekes River.

4.3. Characteristics and Mitigation of Snow and Glacier Hazards Along the Highway

During 2001–2020, the snow-covered area ratio within the 10 km buffer showed a slight but statistically insignificant increase, whereas annual maximum snow depth and annual mean snow depth declined significantly during 2000–2018. Annual maximum snow depth reached 22 cm during the observation period. The relatively stable snow-covered area ratio and declining snow depth are not contradictory, as these indicators describe the horizontal extent and vertical thickness of snow cover, respectively. Their differing trends may reflect changes in snow accumulation and ablation and their seasonal and spatial variability, as well as differences in the observation periods and spatial resolutions of the two products [22–24]. Declining snow depth does not necessarily imply reduced avalanche or snowmelt-flood hazards. Avalanche release also depends on local snowpack stratigraphy, short-term snowfall, and warming conditions, whereas snowmelt flooding depends on snow water equivalent and runoff routing [25,26].

The five recorded snowmelt-flood events in Akqi County demonstrate the potential for damage to transportation and other infrastructure. Four occurred in summer (July and August), whereas one occurred in spring (April). As clarified in Section 4.2, these county-level records provide regional context because their hydrological connections to the study highway have not been verified. Where field investigations confirm flood pathways reaching the highway, mitigation options include channel maintenance, obstruction removal, and erosion protection for roadbeds and slopes (Figure 6a,b). The need for flood-control embankments, diversion channels, and energy-dissipation or scour-protection measures should be evaluated through site-specific assessments. Monitoring air temperature, snow depth, meltwater runoff, and river stage can support early warning of flooding during spring and summer snowmelt.



Figure 6. Snowmelt-flood events and avalanche-hazard mitigation measures: (**a**,**b**) mechanical equipment conducting clearing and dredging at hazard-prone sites; (**c**) snow-retaining wall; (**d**) snow fence.

An avalanche is a gravity-driven downslope movement of snow. In the Tianshan Mountains traversed by the China–Kyrgyzstan Highway, cold conditions and relatively shallow snowpacks can promote strong temperature gradients, snow metamorphism, and persistent weak-layer formation [27]. The snow-covered area ratio within the 10 km buffer generally reaches its maximum in winter and spring, while snow depth peaks in February. Engineering approaches to avalanche mitigation include snowpack stabilization, flow interception, diversion, and protection of exposed infrastructure (Figure 6c,d). Supporting structures, such as snow bridges and supporting fences, are primarily installed in starting zones to stabilize the snowpack. Catching dams and snow-retaining mounds can intercept avalanche flow, whereas deflection dams redirect it away from exposed infrastructure. Snow sheds and tunnels provide protection where roads cross avalanche paths. The suitability and design of these measures require site-specific identification of starting zones and runout paths, together with estimates of avalanche volume and impact pressure.

Glacier surging involves episodes of accelerated glacier flow separated by longer periods of relatively slow motion [28]. Four surge-type glaciers were identified outside the highway's 10 km buffer in the Kungey Mountains. Regional observations include glacier advance, surface-elevation changes, moraine displacement, and crevasse development, with documented surge durations of approximately 3–9 years (Section 4.2). These records provide regional context but do not demonstrate a direct threat to the highway. The mechanisms controlling these surges were not examined in this study. Approximately 75% of glaciers along the highway are smaller than 0.5 km^2; however, glacier size alone is insufficient to determine ice-avalanche susceptibility. Monitoring priorities should reflect the presence of unstable ice on steep slopes or in hanging glaciers, potential rock-slope failures, and continuous propagation pathways to the highway. Where such connections are confirmed, glacier-motion monitoring, time-lapse cameras, and early-warning systems can support hazard management. The selection of interception or energy-dissipation structures requires site-specific estimates of the likely movement type, volume, and impact magnitude.

GLOFs are sudden floods resulting from the rapid release of water stored in glacial lakes. Potential triggers and contributing processes include ice avalanches, landslides, extreme precipitation, increased meltwater inflow, and degradation of buried ice within moraine dams [29]. The ten GLOF events documented at seven lakes during 1974–2019 provide regional evidence of flood processes and impacts; they do not constitute ten confirmed events affecting the study highway. Between 1990 and 2018, glacial-lake number increased by 13, accompanied by an increase in total lake area. Two lakes adjacent to the highway, GL077727E41869N and GL077715E41879N, expanded over this period and warrant targeted assessments of their outlets, dam conditions, and potential drainage pathways to the highway. Common GLOF mitigation measures include controlled lake drainage, dam reinforcement, river embankments, and monitoring and early-warning systems (Figure 7). The suitability of drainage or dam reinforcement should be evaluated through site-specific assessments of lake and dam stability, downstream connectivity, and engineering feasibility, rather than proximity to the highway alone. Where flood pathways to the highway are confirmed, monitoring should cover both lake conditions and downstream road crossings.

Interactions among snow cover, glaciers, and glacial lakes may link individual hazards into cascading processes. Rapid snowmelt and glacier ablation can increase water inflow to channels and lakes; where inflow exceeds drainage capacity, rising water levels may increase flood hazards. Degradation of buried ice may also weaken moraine complexes and alter lake drainage conditions. The Toguz-Bulak case described in Section 4.2 provides regional evidence linking glacier meltwater supply, moraine degradation, lake outburst, and downstream infrastructure damage. Following an outburst, floodwater may entrain sediment as it propagates through erodible channels, further increasing impacts on bridges, roadbeds, and drainage structures. These pathways highlight the need to consider upstream hazard sources, intermediate water storage, and downstream propagation together. Other potential hazard cascades include snow avalanches, ice avalanches, or rock–ice avalanches entering lakes and generating displacement waves that may cause overtopping or dam erosion. Where glaciers and lakes are directly connected, glacier surging may also modify lake geometry and drainage conditions. Except for the documented regional case described above, these pathways represent plausible mechanisms rather than verified cascading events affecting the study highway. Their relevance to specific highway sections requires confirmation of source conditions and continuous propagation pathways.

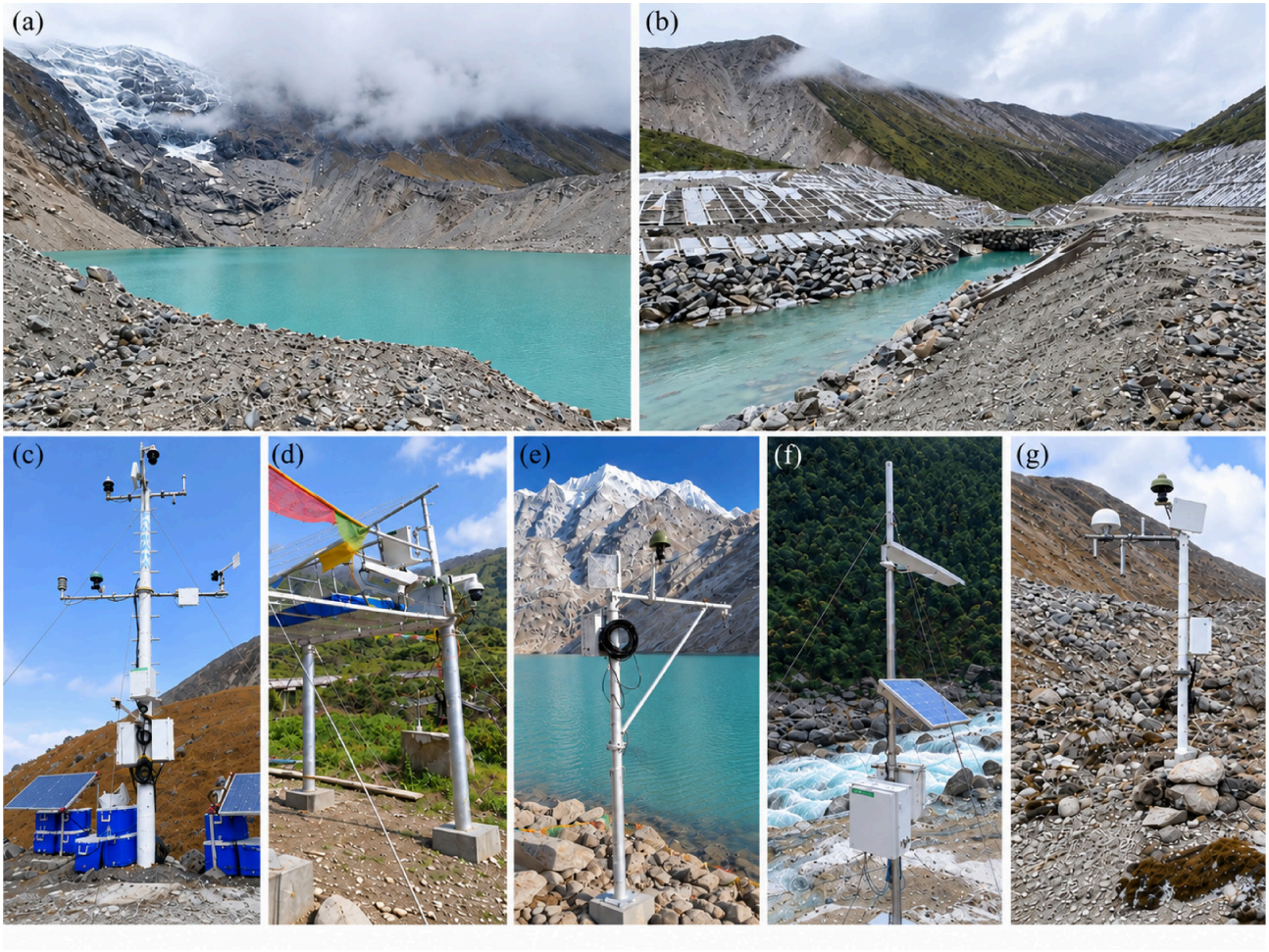

Figure 7. Mitigation measures for glacial lake outburst floods: (**a**) artificial drainage of moraine-dammed lakes; (**b**) reinforcement of moraine dams; (**c**) meteorological monitoring in glacial-lake areas; (**d**) river-channel monitoring; (**e**) lake-level monitoring; (**f**) downstream water-level monitoring; (**g**) moraine-ridge monitoring. All photographs were modified from [30].

4.4. Integrated Susceptibility Assessment and Risk Management

The construction and operation of highway infrastructure in areas with concentrated snow cover, glaciers, and glacial lakes may be affected by snow- and glacier-related hazards and engineering challenges. Based on corridor conditions, historical records, and regional evidence, five snow- and glacier-related hazard types were considered: avalanches, snowmelt floods, glacier surges, GLOFs, and glacier avalanches. These include both documented regional hazards and potential processes requiring local verification. Using the framework described in Section 3.3, we conducted an integrated assessment within the 10 km buffer zone along the China–Kyrgyzstan Highway.

Moderate susceptibility predominates within the assessed corridor, while high susceptibility is concentrated in specific highway sections. High- and moderate-susceptibility zones together account for approximately 80% of the study area (Figure 8). Spatially, the susceptibility classes form a belt-like pattern along the highway that closely follows the mountainous topography. The distribution of snow cover, glaciers, and glacial lakes creates locally concentrated high-susceptibility belts that may pose potential threats to highway construction and operational safety.

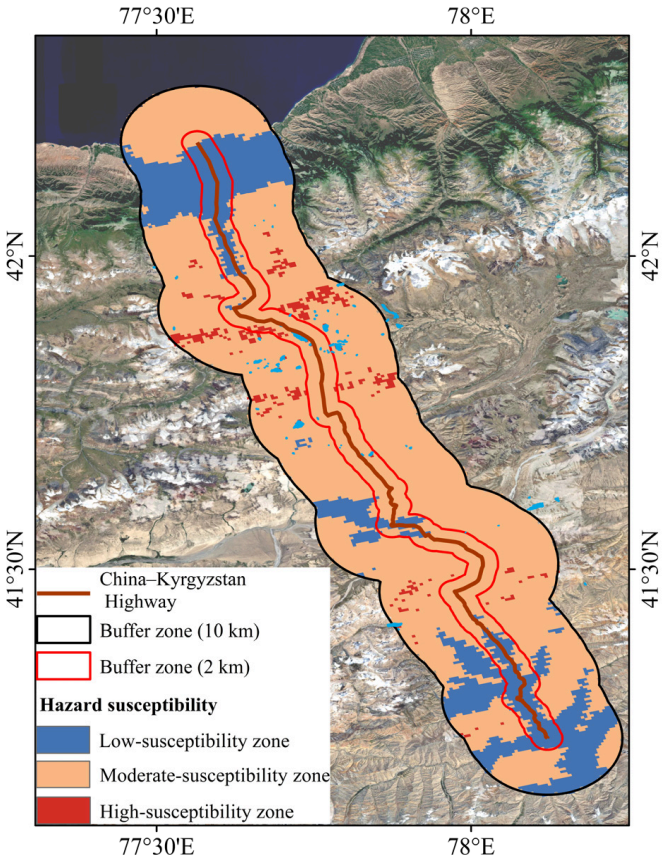

Figure 8. Susceptibility to snow- and glacier-related hazards within the 10 km buffer zone along the China–Kyrgyzstan Highway.

High-susceptibility zones account for approximately 2% of the study area. Although limited in total extent, they are strongly concentrated in two highway sections located approximately 35–64 km and 92–101 km from the starting point. These sections are characterized by complex terrain and widespread snow cover and glaciers, which should therefore be prioritized for field investigation and monitoring (Figure 9a,b). Moderate-susceptibility zones are the most extensive, accounting for approximately 78% of the study area, and include areas where thermokarst lakes and ponds are concentrated (Figure 9c,d). Their extensive distribution warrants systematic inspection of drainage conditions and potential connections between upstream sources and the highway. Low-susceptibility zones generally have gentler terrain and lie farther from major areas of snow accumulation and glacier cover, so preventive maintenance should be emphasized in these zones.

For the priority sections approximately 35–64 km and 92–101 km from the highway starting point, field surveys should verify potential connections between snow-covered slopes, glacier bodies, upstream lakes, and the road. Monitoring should target the identified hazards, including snowpack conditions, changes in glacier surface velocity, lake levels, and downstream discharge. The outlets and drainage paths of the expanding glacial lakes GL077727E41869N and GL077715E41879N should be inspected. If drainage pathways to the highway are confirmed, monitoring of the lakes and downstream channels should inform early warning and mitigation planning. Moderate-susceptibility sections require inspection and maintenance of bridges, culverts, drains, and erosion-prone crossings, particularly during melt periods. Low-susceptibility sections should receive routine snow clearance and drainage maintenance. Protective measures should be selected following site-specific verification of hazard sources, propagation pathways, and expected impacts.

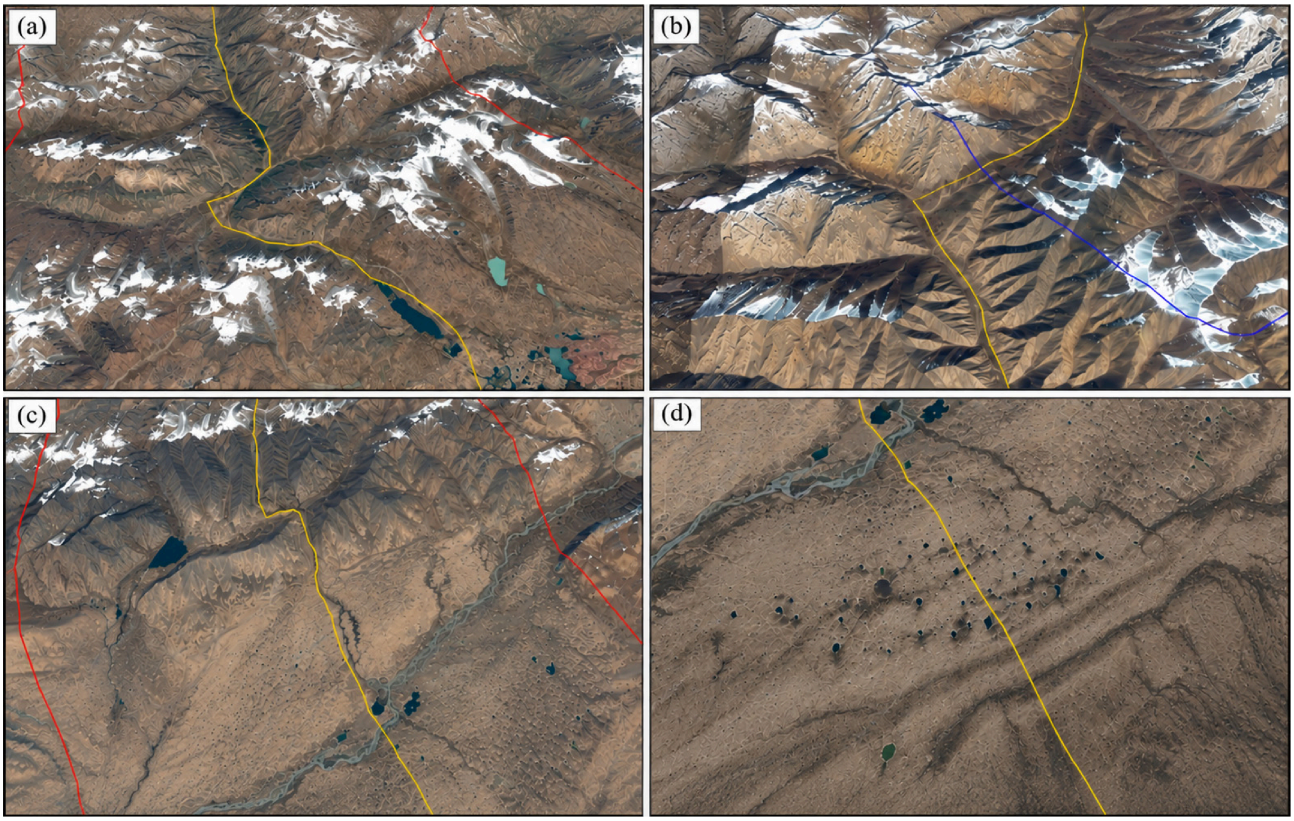

Figure 9. Photographs of snow- and glacier-hazard-prone areas within the 10 km buffer zone along the China–Kyrgyzstan Highway (yellow line): (**a**) approximately 35–64 km from the highway starting point; (**b**) approximately 92–101 km from the highway starting point; (**c**) glacial lakes located very close to the highway; (**d**) thermokarst lakes and thermokarst ponds.

The fixed 10 km buffer provides a consistent framework for corridor-scale assessment, but proximity alone does not establish a hazard propagation pathway. Glaciers or lakes within the buffer may be separated from the highway by drainage divides, whereas sources outside it may affect the highway through connected upstream catchments and river channels. The assessment may therefore omit distant but connected sources and include nearby sources with limited influence on the highway. Further screening should consider catchments upstream of highway crossings and trace potential pathways from glacier and lake sources through tributaries and main channels to bridges, culverts, and valley-side road sections. For avalanches and other mass movements, slope geometry and runout paths must also be examined. The four surge-type glaciers in the Kungey Mountains provide regional context, but their influence on the study highway remains unconfirmed without evidence of a continuous propagation pathway. Similarly, the regional GLOF cases discussed in Section 4.2 illustrate possible downstream impacts rather than establish direct exposure of the study highway. As catchment delineation and channel-based propagation analysis were not undertaken in this study, the susceptibility map should be interpreted as a screening result within the defined buffer. Subsequent assessments should extend the investigation to external glacier and glacial-lake sources in catchments draining toward the highway and verify their connections to exposed infrastructure.

5. Conclusions

Using glacier and glacial-lake inventories, satellite-derived snow products, and compiled historical hazard records, this study examined changes in snow-covered area ratio, snow depth, glaciers, and glacial lakes and assessed associated hazard susceptibility within a

10 km buffer on each side of the Baryskoon–Bedel Border Port Highway (China–Kyrgyzstan Highway). Historical records provided regional context for identifying potential hazard processes, while the integrated susceptibility assessment identified areas requiring priority investigation. The main conclusions are as follows:

(1) The snow-covered area ratio within the 10 km buffer remained relatively stable during 2001–2020, with a period mean of 10.33%. In contrast, annual maximum snow depth and annual mean snow depth declined significantly during 2000–2018. Annual maximum snow depth ranged from 6.6 to 22 cm, with a period mean of 12.54 cm, while annual mean snow depth ranged from 1.66 to 3.36 cm, averaging 2.16 cm. Snow depth exhibited a pronounced seasonal cycle: snow accumulation began in September–October, snow depth peaked in February, declined markedly from March to May, and reached its minimum in August. These seasonal conditions suggest that avalanche and blowing-snow hazards warrant attention in winter, while snowmelt-flood hazards require particular attention in spring and summer.

(2) In 2002, 337 glaciers were identified within the 10 km buffer, of which 252 (75%) were smaller than 0.5 km^2. Within the 2 km buffer, 71 glaciers were identified, with a mean area of 0.39 km^2. Between 2002 and 2022, the glacier number decreased by 66, while total glacier area decreased by 24.12 km^2, corresponding to a mean annual area reduction of 0.914% relative to the 2002 area. No surge-type glaciers were identified within the 10 km buffer, but four were identified outside it in the Kungey Mountains. Their potential influence on the highway remains unconfirmed because connecting hazard propagation pathways have not been established.

(3) In 2018, 77 glacial lakes were identified within the 10 km buffer, forming spatial clusters dominated by small lakes, with 70 of the 77 lakes having an area of less than 0.5 km^2. Within the 2 km buffer, 31 glacial lakes were identified, with a mean area of 0.11 km^2. 2 lakes adjacent to the highway, GL077727E41869N and GL077715E41879N, warrant priority investigation of their stability and potential drainage pathways to the road. Between 1990 and 2018, lake number and total area increased by approximately 20% and 17%, respectively. Ten regional GLOF events were documented during 1974–2019, illustrating potential flood processes and impacts without establishing direct hydrological connections to the study highway.

(4) Moderate susceptibility to snow- and glacier-related hazards predominates within the 10 km buffer, covering approximately 78% of the study area. High-susceptibility zones account for approximately 2% and are concentrated along highway sections approximately 35–64 km and 92–101 km from the starting point. These zones coincide with concentrations of snow cover, glaciers, and glacial lakes in areas of pronounced topographic relief. The susceptibility map provides screening-level guidance for prioritizing field investigations and monitoring. Further field investigations, geotechnical engineering assessments, and verification through monitoring are required to confirm hazard sources, propagation pathways, and potential impacts before conclusions about highway engineering safety can be drawn or site-specific mitigation measures selected.

Author Contributions: Conceptualization, K.Z., and P.W.; methodology, K.Z. and H.L.; software, H.L.; formal analysis, K.Z., H.L. and Y.M.; investigation, K.Z., Y.M. and Y.L.; data curation, Y.L. and F.Y.; writing—original draft preparation, K.Z.; writing—review and editing, K.Z., H.L., Y.M., Y.L., F.Y. and P.W.; visualization, H.L. and F.Y.; supervision, P.W.; funding acquisition, P.W. All authors have read and agreed to the published version of the manuscript.

Funding: This research was jointly funded by the Talent Project of Northwest Minzu University (xbmuyjrc2023018), the Major Science and Technology Projects of Gansu Province (23ZDFA017),the National Natural Science Foundation of China (42371148; 42501170; U25A20788), the Science and

Technology program of Gansu Province (25JRRA542; 25JRRA995), and the Program of the State Key Laboratory of Cryospheric Science and Frozen Soil Engineering, NIEER, CAS (CSFSE-TZ-2512).

Data Availability Statement: The datasets used in this study are publicly available from their original repositories or associated publications. The Long-term Series of Daily Global Snow Depth Dataset (1980–2018) was obtained from the National Tibetan Plateau Data Center (https://doi.org/10.11888/Snow.tpdc.270925). The Belt and Road Snow Area Proportion Daily Data Product Dataset, derived from MOD09GA surface reflectance, was obtained from the National Cryosphere Desert Data Center. Glacier outlines were obtained from the Randolph Glacier Inventory (RGI v7.0) and the glacier inventory of four Central Asian countries published by Guo et al. (2024) (https://doi.org/10.57760/sciencedb.j00001.01043); the outlines used for the corridor correspond to 2002 and 2022, respectively. Glacial-lake outlines for 1990 and 2018 were obtained from the Glacial Lake Inventory of High Mountain Asia, distributed by the National Cryosphere Desert Data Center. Snowmelt-flood and glacial lake outburst flood records were obtained from the historical flood-disaster dataset for the Tibetan Plateau and surrounding mountain regions (1950–2023), while surge-type glacier data were obtained from the inventory of surge-type glaciers in High Mountain Asia.

Conflicts of Interest: Author Yaozheng Luan was employed by CCCC Highway Consultants Co., Ltd. The remaining authors declare that the research was conducted in the absence of any commercial or financial relationships that could be construed as a potential conflict of interest.

References

1. Yao, T.; Zhang, T.; Wang, W.; Zhang, G.; Liu, S.; An, B. Glacial lake change and outburst risk assessment on the Asian Water Tower. *Adv. Earth Sci.* **2025**, *40*, 221–227.
2. Yao, J.; Chen, Y.; Guan, X.; Zhao, Y.; Chen, J.; Mao, W. Recent climate and hydrological changes in a mountain–basin system in Xinjiang, China. *Earth-Sci. Rev.* **2022**, *226*, 103957. [CrossRef]
3. Chen, Y.; Li, Y.; He, B.; Wang, Y.; Li, Z.; Fang, G.; Zhu, C.; Chen, Y. Enhanced spring warming in Central Asia and its ecohydrological impacts. *Chin. Sci. Bull.* **2026**, *71*, 3849–3855. [CrossRef]
4. Dahe, Q. *Scientific Assessment Report on Climate Change in Xinjiang*; Science Press: Beijing, China, 2023.
5. Lin, Z.; Niu, F.; Luo, J.; Liu, M.; Yin, G. Thermal regime at bottom of thermokarst lakes along Qinghai-Tibet engineering corridor. *Earth Sci.* **2015**, *40*, 179–188.
6. Mu, Y.; Ma, W.; Li, G.; Niu, F.; Liu, Y.; Mao, Y. Impacts of supra-permafrost water ponding and drainage on a railway embankment in continuous permafrost zone, the interior of the Qinghai-Tibet Plateau. *Cold Reg. Sci. Technol.* **2018**, *154*, 23–31. [CrossRef]
7. Yang, R.; Zhang, T.; Zhu, L.; Ju, J. Laigu glacial lake variation and its outburst flood risk in southeast Tibetan Plateau. *J. Glaciol. Geocryol.* **2019**, *41*, 1171–1180.
8. Duo, C. Study on avalanche hazards and response measures in Tibet area. *Plateau Mt. Meteorol. Res.* **2022**, *42*, 117–126.
9. Cheng, G.; Li, X.; Jin, H. Cryospheric engineering helps infrastructure construction for interconnection. *Bull. Chin. Acad. Sci.* **2020**, *35*, 431–438.
10. Shugar Dan, H.; Aaron, B.; Haritashya Umesh, K. Rapid worldwide growth of glacial lakes since 1990. *Nat. Clim. Change* **2020**, *10*, 939–945. [CrossRef]
11. Taylor, C.; Robinson, T.R.; Dunning, S. Glacial lake outburst floods threaten millions globally. *Nat. Commun.* **2023**, *14*, 487. [CrossRef] [PubMed]
12. Mirlan, D.; Chiyuki, N.; Andreas, K. Formation and outburst of the Toguz-Bulak glacial lake in the northern Teskey Range, Tien Shan, Kyrgyzstan. *Geosciences* **2020**, *10*, 468. [CrossRef]
13. Mirlan, D.; Chiyuki, N. Formation, evolution, and drainage of short-lived glacial lakes in permafrost environments of the northern Teskey Range, Central Asia. *Nat. Hazards Earth Syst. Sci.* **2021**, *21*, 2245–2256. [CrossRef]
14. Ashim, S.; Cook, K.; Kant, R.S. The Sikkim flood of October 2023: Drivers, causes, and impacts of a multihazard cascade. *Science* **2025**, *387*, eads2659. [CrossRef] [PubMed]
15. Chen, M.; Chen, Y.; Fang, G. Risk assessment of glacial lake outburst flood in the Central Asian Tienshan Mountains. *npj Clim. Atmos. Sci.* **2024**, *7*, 209. [CrossRef]
16. Shen, Y.; Su, H.; Wang, G.; Mao, W.; Wang, S. The response of glaciers and snow cover to climate change in Xinjiang (II): Hazards effects. *J. Glaciol. Geocryol.* **2013**, *35*, 1355–1370.
17. Guo, Z.; Yao, X.; Cheng, Y.; Liu, Y. *A Dataset of Glacier Inventory in Four Central Asian Countries During 2022–2023*; Science Data Bank: Beijing, China, 2024.

18. Khadka, N.; Chen, X.; Nie, Y.; Thakuri, S.; Zheng, G.; Zhang, G. Evaluation of glacial lake outburst flood susceptibility using multi-criteria assessment framework in Mahalangur Himalaya. *Front. Earth Sci.* **2021**, *8*, 601288. [CrossRef]
19. Rinzin, S.; Zhang, G.; Wangchuk, S. Glacial lake area change and potential outburst flood hazard assessment in the Bhutan Himalaya. *Front. Earth Sci.* **2021**, *9*, 775195. [CrossRef]
20. Rafique, A.; Dasti, M.Y.S.; Ullah, B. Snow avalanche hazard mapping using a GIS-based AHP approach: A case of glaciers in Northern Pakistan from 2012 to 2022. *Remote Sens.* **2023**, *15*, 5375. [CrossRef]
21. Daiyrov, M.; Kattel, D.B.; Narama, C.; Wang, W. Evaluating the variability of glacial lakes in the Kyrgyz and Teskey ranges, Tien Shan. *Front. Earth Sci.* **2022**, *10*, 850146. [CrossRef]
22. Tao, C.; Hao, X.; Dai, L.; Li, H.; Huang, X.; Lin, X. Snow Cover Variation and Its Impacts over the Qinghai-Tibet Plateau. *Bull. Chin. Acad. Sci.* **2019**, *34*, 1247–1253.
23. Zhao, Q.; Hao, X.; Wang, J.; Luo, S.; Shao, D.; Li, H.; Feng, T.; Zhao, H. Snow Cover Phenology Change and Response to Climate in China during 2000–2020. *Remote Sens.* **2022**, *14*, 3936. [CrossRef]
24. Dai, L.; Che, T.; Ding, Y.; Hao, X. Evaluation of snow cover and snow depth on the Qinghai-Tibetan Plateau derived from passive microwave remote sensing. *Cryosphere* **2017**, *11*, 1933–1948. [CrossRef]
25. Hao, J.; Cui, P.; Zhang, X.; Li, L. The triggering mechanisms for different types of snow avalanches in the continental snow climate of the central Tianshan Mountains. *Sci. China Earth Sci.* **2022**, *65*, 2308–2321. [CrossRef]
26. Wang, J.; Li, H.; Hao, X. Responses of snowmelt runoff to climatic change in an inland river basin, Northwestern China, over the past 50 years. *Hydrol. Earth Syst. Sci.* **2010**, *14*, 1979–1987. [CrossRef]
27. Hao, J.; Li, L. Research progress and prospect of snow avalanche disaster prevention and control. *J. Glaciol. Geocryol.* **2022**, *44*, 762–770.
28. Guo, W.; Zhang, Z.; Wu, K.; Liu, S.; Shangguan, D.; Xu, J.; Jiang, Z.; Wang, X. Progress of surge glacier research. *J. Glaciol. Geocryol.* **2022**, *44*, 954–970.
29. Zhang, T.; Wang, W.; Gao, T.; An, B.; Shang, X. Review of glacial lake outburst flood events in High Mountain Asia. *J. Glaciol. Geocryol.* **2021**, *43*, 1365–1381.
30. Zhang, T. *Glacial Lake Changes, Outburst Hazard Risk Assessment and Response in the Third Pole*; Lanzhou University: Lanzhou, China, 2025.

Disclaimer/Publisher's Note: The statements, opinions and data contained in all publications are solely those of the individual author(s) and contributor(s) and not of MDPI and/or the editor(s). MDPI and/or the editor(s) disclaim responsibility for any injury to people or property resulting from any ideas, methods, instructions or products referred to in the content.